Tianjin Daxue Xuebao (Ziran Kexue yu Gongcheng Jishu Ban)/
Journal of Tianjin University Science and Technology
ISSN (Online):0493-2137
E-Publication: Online Open Access
Vol: 57 Issue: 03:2024
DOI: 10.5281/zenodo.10792408

EXPERIMENTAL INVESTIGATION ON THE BEHAVIOR OF HIGH-STRENGTH SELF-COMPACTED REINFORCED CONCRETE SLENDER BEAMS UNDER STATIC LOADING

MOHAMED. O. ELSIBAEY
Department of Civil Engineering, Faculty of Engineering, Aswan University, Egypt.

MONA SALEH
Department of Civil Engineering, Faculty of Engineering, Aswan University, Egypt.

ZAKARIA. H. AWADALLAH
Department of Civil Engineering, Al-Azhar University, Egypt.

ABDO KHALAF
Department of Civil Engineering, Al-Azhar University, Egypt.

AYMAN OTHMAN
Department of Civil Engineering, Faculty of Engineering, Aswan University, Egypt.

MOHAMED ZAKARIA
Department of Civil Engineering, Faculty of Engineering, Aswan University, Egypt.

Abstract

In this study, I conducted an experimental investigation to understand the behaviour of high-strength, self-compacted reinforced concrete beams under static loading. Simply supported, slender concrete beams with different parameters were tested. The investigated beams were 100 × 750 mm in size and 4000 mm long and were tested under 4-point loading. The main parameters investigated were the web reinforcement ratio, the concrete strength and the span to depth ratio (a/d). The effects of these parameters were investigated on mid-span deflection, lateral torsion, concrete strains, steel strains, failure modes and crack patterns. It was found that the main reinforcement ratio and the ratio of shear span to shear depth have a remarkable influence on the mid-span deflection of slender beams. As the main reinforcement ratio increases, the mid-span deflection of slender beams generally decreases. It was found that an increase in concrete strength leads to a 20% reduction in mid-span deflection for B6 at =55 MPa compared to B2 at =30 MPa. The effect of principal reinforcement ratio on the cracking pattern of slender beams is significant and increasing the principal reinforcement ratio leads to a more controlled and tighter cracking pattern. Higher concrete strength is better able to resist tensile stresses, resulting in smaller crack widths and fewer cracks overall. A higher ratio between shear span and shear depth results in a more distributed and wider crack pattern.

Keywords: High-Strength Self-Compacted, Slender Beams, Static Load.

List of Symbols

λ	Normalized slenderness ratio.	M_{bcr}	Critical buckling moment.
$C1$	Factor determining the load type	M_u	Maximum momentary capacity.
$C2$	Factor determining the end condition of the beam	M_{uf}	Ultimate flexural failure moment that was calculated.
Ec	Concrete's elastic modulus.	η	Factor of the moment reduction.
R	Factor of flexional resistance.	λ^{-}	Moderated slenderness ratio.
α	Effective flexural rigidity coefficient.	B	Beam width.

Tianjin Daxue Xuebao (Ziran Kexue yu Gongcheng Jishu Ban)/
Journal of Tianjin University Science and Technology
ISSN (Online):0493-2137
E-Publication: Online Open Access
Vol: 57 Issue: 03:2024
DOI: 10.5281/zenodo.10792408

β	Effective torsional stiffness coefficient.	D	Beam depth.
d	The beam's effective depth.	f_{cu}	Concrete's compressive strength.
L	Length of beam.	*a/d*	Span-to-depth ratio.
b	The effective width of a beam	SCC	Self-compacted concrete

1. INTRODUCTION

Concrete is one of the most important environmentally friendly materials and is preferred worldwide for the construction of large buildings and infrastructure. Mega-reinforced concrete buildings, residential buildings, road pavements, highway bridges and water-bearing structures are all testaments to the use and versatility of concrete. A monolithic set of "members" in reinforced concrete structures act together to support the loads acting on the structure. [1]. One of the primary structural components that allows loads to be carried from the slabs to the columns is the reinforced concrete beam. The main types of RC beams include traditional beams, deep beams and slender beams [2], all of which have their own unique behavioral characteristics and design considerations. It is important to carefully consider the appropriate beam type for a particular application and design the beam accordingly to ensure its safe and efficient performance. Shallow beams are typically designed to resist bending stresses, whereas slender beams and deep beams also need to consider the effects of shear stresses. Slender beams are more susceptible to buckling and other stability issues, while deep beams are more susceptible to shear failure and cracking. The appropriate design of each type of beam depends on various factors, such as the loading conditions, the dimensions of the beam and the properties of the materials used. Numerous researchers have studied the behavior of deep RC beams [3-12]. ACI 318 defines deep RC beams as those with ($a/d \leq 2$) that are loaded on one side and supported on the other. According to ACI 318 Building Code (ACI Committee 318 2008) [13], [14] the strut and tie method can be used for the construction of deep beams. [4, 15-17].

According to ACI 318-08, members with concentrated forces that are within twice the depth of the member from the bearing or members with a clear span that does not exceed four times their depth are classified as deep beams.

It is generally accepted that the ratio of shear span to effective depth (a/d) is the most important factor influencing the behavior of reinforced concrete beams [18-20]. It has long been known that the ratio (a/d) plays an important role in the load transfer characteristics of deep beams. The nonlinear behavior of deep reinforced concrete beams and slender beams poses a great challenge to researchers. In addition, previous studies have not considered all the important aspects that influence the behavior of RC deep beams. Slender beams have not yet been sufficiently discussed.

Slender RC beams behave quite differently from conventional and deep beams. The idea of this research came to study the behavior of slender beams because they have not been studied sufficiently by researchers due to the difficulty of understanding them and their uses.

Tianjin Daxue Xuebao (Ziran Kexue yu Gongcheng Jishu Ban)/
Journal of Tianjin University Science and Technology
ISSN (Online):0493-2137
E-Publication: Online Open Access
Vol: 57 Issue: 03:2024
DOI: 10.5281/zenodo.10792408

The current ACI, EGY, BS and IS codes [13, 21-23] state that slenderness depends only on the beam dimensions. However, other (different) studies and researchers conclude that the slenderness of beams depends on a number of variables, including the ratio between shear span and depth, concrete compressive strength and reinforcement ratio, and beam size.

In extremely slender beams, sudden instability can occur as a type of failure. The problematic issue of the shear and bending strength of RC beams, especially of shear-critical components such as slender RC beams, is still being discussed in academic circles. Their non-linear behavior which is influenced by many parameters, is the cause of this. To make matters worse, shear forces always occur in conjunction with other loads, such as bending, axial load and occasionally torsion. Since shear failure can occur suddenly and have catastrophic consequences, accurate prediction of shear capacity is essential.

The lateral stability of reinforced concrete beams was investigated experimentally and analytically by **Hansell and Winter (1959)**. They tested 5 different groups of beams. They wanted to find out whether increasing L/b ratios would lead to a possible reduction in the bending capacity of reinforced concrete beams. The authors created a composite measure of slenderness ratio $(L/b)*(d/b) = Ld/b^2$, where L, b and d are the span, width and effective depth of the rectangular beam, respectively. They concluded that all specimens reached their maximum flexural strength before buckling in torsion and that they failed under the pressure of bending moments after the tensile reinforcement had yielded. They emphasized that any failure of a beam was caused by bending and not by instability [24].

Siev (1960) investigated the lateral buckling of reinforced concrete beams with initial deficiencies. His experimental investigations led him to the conclusion that, besides the ratio L/b, the ratio d/b and the percentage of reinforcement also have an influence on the critical buckling moment of RC beams. He also proved that beams with a concrete quality of more than 50 MPa are more likely to break due to instability than beams with a lower concrete quality [25].

Sant and Bletzacker (1961) examined four groups of beams, and their results showed large, significant differences. For example, the experimental buckling moment of beam B30-2 was 54% higher than the experimental value obtained when its counterpart, beam 30-1, was tested. The relationship between the experimental and predicted buckling moment in the beam 36, beam 30 and beam 24 specimen groups indicates differences in the test results of the companion beams. Since beams 12-1 and 12-2 did not suffer from lateral buckling [26].

Revathi and Menon (2011) reported their findings from fifteen experimental trials conducted on rectangular slender RC beams. They found that the theoretical models currently used to calculate the ultimate moment capacity and failure mechanism have limited applicability. Their theoretical model for predicting the critical buckling moment (M_{bcr}) for slender rectangular beams that are both single and double reinforced has been

Tianjin Daxue Xuebao (Ziran Kexue yu Gongcheng Jishu Ban)/
Journal of Tianjin University Science and Technology
ISSN (Online):0493-2137
E-Publication: Online Open Access
Vol: 57 Issue: 03:2024
DOI: 10.5281/zenodo.10792408

improved. This approach aims to address the shortcomings and limitations of the earlier study by Revathi and Menon. To evaluate M_{bcr} for reduced bending strength and rectangular beams $M_u = \eta M_{uf}$ for moderately slender beams, they conducted experiments on moderately and very slender RC beams and provided expressions.

They developed a limiting value for the slenderness ratio (λ) and showed that a variety of slenderness constraints are possible for different groups of design variables. They proposed an equation to determine the slenderness modulus of the beams.

$$\lambda = \frac{C1}{10C2}\frac{Ec}{R}\sqrt{\alpha\beta}\ldots\ldots\ldots\ldots \rightarrow Equation(1)$$

Additionally, they enhanced the slenderness ratio $\lambda^{-} = \sqrt{M_{uf} / M_{bcr}}$. Slenderness effects - the interaction between bending stress and unstable failure modes - were found to reduce the flexural capacity of beams with λ^{-} in the range of 0.5–1.27. With respect to λ^{-}, an equivalent formula for the moment reduction factor $\eta = M_u/M_{uf}$ was established.

Furthermore, the expression was confirmed by existing experimental data, and they proposed $\lambda^{-} \leq 1.0$ as the basis for preventing abrupt failure of instability in slender RC beams. Against this background, they proposed a simple formula for the limiting slenderness ratio of Ld/b^2 [27].

Nine Slender HSC beams with an effective length of 900 mm and a constant dimension of 125 x 130 mm were tested by **B.K.Kolhapure in 2013**. The web reinforcement ratio and longitudinal reinforcement ratio were the parameters studied to investigate the shear behaviour of beams with maximum and minimum web reinforcement as per IS and ACI codes. The experimental results obtained are compared with the theoretical values according to the code. These data suggest that a variety of factors, including the percentage of longitudinal and shear reinforcement, the concrete grade, the depth of the beam and the ratio of shear span to depth (*a/d* ratio>2), influence the shear behaviour of reinforced concrete beams.

We can deduce that the shear collapse is sudden, very explosive, and brittle. The load carrying capacity rose with decreasing shear reinforcement spacing (75 mm) and declined with increasing shear reinforcement spacing (225, 300 mm). Small deflection, lack of ductility, and catastrophic failure are the characteristics of shear failure. [28]**.**

2. MATERIALS AND METHODS

To achieve the research objectives, ten slender reinforced concrete beams were tested according to the test program. The control beam concrete was produced from traditional strength concrete. The nine remaining beams (The remaining nine beams) were made of high-strength concrete. The control beam, which was classified as a non-slender beam, had a width of 120 mm and a total span of 2000 mm. The other beams tested had a width of 100 mm and a total span of 4000 mm. The nine beams tested were divided into three groups. Each group contained three samples that differed in one of the influencing

Tianjin Daxue Xuebao (Ziran Kexue yu Gongcheng Jishu Ban)/
Journal of Tianjin University Science and Technology
ISSN (Online):0493-2137
E-Publication: Online Open Access
Vol: 57 Issue: 03:2024
DOI: 10.5281/zenodo.10792408

parameters. The first group contained beams 2, 5 and 6, which differed in concrete strength of 30, 45 and 55 MPa respectively. In order to understand the effect of the main reinforcement ratio, beams 3, 4 and 7 were examined. They differed in the number and diameter of the steel bars and in the number of rows. Finally, the third group was used to investigate the effect of a/d. Three values of a/d, namely 1.75, 2 and 2.22, were compared with each other. All details of the test program are shown in **Table 1.**

Table 1: Details of the tested program.

Beam Label	*B×D×L* (mm)	*a/d*	$f_{cu\ design}$ (MPa)	Main Reinforcement	Secondary Reinforcement	Type
Beam 1	120×750×2000	1	25	4 Ø16	4 Ø16	Non-Slender
Beam 2	100×750×4000	2.22	30	4 Ø16	4 Ø16	Slender
Beam 3	100×750×4000	2	55	4 Ø12	4 Ø12	Slender
Beam 4	100×750×4000	2	55	6 Ø12	6 Ø12	Slender
Beam 5	100×750×4000	2.22	45	4 Ø16	4 Ø16	Slender
Beam 6	100×750×4000	2.22	55	4 Ø16	4 Ø16	Slender
Beam 7	100×750×4000	2	55	4 Ø10	4 Ø10	Slender
Beam 8	100×750×4000	1.75	55	6 Ø12	4 Ø12	Slender
Beam 9	100×750×4000	2	55	6 Ø12	4 Ø12	Slender
Beam 10	100×750×4000	2.22	55	6 Ø12	4 Ø12	Slender

- Beams 2,5 and 6 are varied in the concrete strength.
- Beams 3,4 and 7 are varied in the main reinforcement ratio.
- Beams 8,9 and 10 are varied in *a/d*.
- $Long.Reinf_{comp}$ Longitudinal compression steel reinforcement.
- $Long.Reinf_{ten}$ Longitudinal tension steel reinforcement.

2.1 Materials

Ordinary Portland cement (Assiut cement) of grade 32.5 was used for the production of concrete. To assure that the cement used in the studies was fresh and free of lumps and other foreign matter, it was stored in a dry environment. **Table 2** shows the test results for ordinary portland cement.

Table 2: All test results of Ordinary Portland Cement

% Of Reserved on Sieve No. 170		4.7
First time setting times (min)		73
Final time setting times (min)		217
Compressive strength of mortar (MPa)	3 days	19.55
	7 days	29.14

Tianjin Daxue Xuebao (Ziran Kexue yu Gongcheng Jishu Ban)/
Journal of Tianjin University Science and Technology
ISSN (Online):0493-2137
E-Publication: Online Open Access
Vol: 57 Issue: 03:2024
DOI: 10.5281/zenodo.10792408

Clean, fine aggregate was used. Before use, the sand was cleaned and left to dry in the open air. The sand was washed and dried outdoors before use. Sieves were used to maintain the quality of the sand. Fine sieves were used to remove very fine material from the mixture according to ECP. Round, well-graded coarse aggregates in two sizes (0 and 10 mm) were used in the mixture. As indicated in **Table 3,** reinforcing steel with a typical yield strength of 420 MPa for the longitudinal reinforcement and 250 MPa for the stirrups was used.

Drinking water was used for the mixtures. At low water/cement ratios, the superplasticizer ensures that the concrete is sufficiently workable. (see Fig. 1).

Fig.1: Weigh the components of the concrete mix.

Table 3: The experimental specimens' steel bar's material properties

Diameter (mm)	Strength of yield f_y (MPa)	Ultimate strength f_u (MPa)	Ultimate strain δ (%)
8	274	426	23.6
10	415.17	686	15.25
12	436	672	17.6
16	438	658	16.3

2.2 Mix design.

In the concrete research laboratory of Assiut College (C.R.L.), the mixtures used to produce the test specimens were developed using trial mixtures. The following are the mixes' details: -

Two different normal strength concrete mixes were used in this experimental investigation.

After 28 days, trial mixes were used to achieve the target cylinder compressive strength of 25 and 30 MPa. **Table 4** shows the weight proportions of the mix required to achieve the target cube compressive strength in one cubic meter of concrete.

2.2.1 High Self-Compacted Strength Concrete

High-strength concrete (HSC) is defined by ACI Committee 318 (ACI 318) as concrete with a cylinder compressive strength greater than 41 MPa. Certain additives, such as Sika ViscoCrete® R4PN, have been added to concrete to create high-strength concrete [29, 30].

Tianjin Daxue Xuebao (Ziran Kexue yu Gongcheng Jishu Ban)/
Journal of Tianjin University Science and Technology
ISSN (Online):0493-2137
E-Publication: Online Open Access
Vol: 57 Issue: 03:2024
DOI: 10.5281/zenodo.10792408

Sika ViscoCrete® R4PN[31] is a very powerful dual-action liquid super-plasticizer that can be used to create concrete that flows easily or as a significant water-reducing agent to encourage the creation of concrete with high strength.

Also, to make self-compacting concrete (SCC), Sika ViscoCrete®-3425 have been added. Sika ViscoCrete®-3425[32] is a third-generation super-plasticizer for homogenous concrete and mortar. It is particularly well suited for producing concrete mixtures that have-to-have strong water reduction, high early strength development, and outstanding flowability. Two different high-strength concrete mixes were used in these tests. Trial mixes were conducted to reach the target cubes compressive strength of 45 and 55 MPa after 28 days.

2.3 Mixing, Placing, and Curing

Although the water-cement ratio was dosed by weight of the mixture, the components of the concrete were dosed independently by weight, using a mechanical scale with a sensitivity of 0.1 kg. Mixing was carried out using a concrete tipping drum mixer. Mixing took five minutes; one minute to mix the dry materials until a uniform color was observed. **(See Fig.1)**

Clean wooden molds were used for casting. All sides of the wooden molds were coated with oil before casting began. The reinforcement cage was prepared and placed in these molds. The concrete was mixed and then immediately poured into the molds, taking into account the reinforcement required for the pour. After removing the wooden molds the next day, a daily curing process of up to 28 days was initiated. After 28 days of casting, the beams were ready for testing, **Fig. 2**. Sixty standard cubes measuring (150 * 150 * 150 mm) were taken during casting, half of which were tested after 7 days and the other half after 28 days.

After 24 hours after casting, all the beams and cubes were demolded and hardened under tapestry sheets to prevent the loss of moisture. After seven and twenty-eight days of water curing the concrete, I examined the standard cubes for compression cubes.

Fig.2: Preparing of casting and curing of the tested beams.

Tianjin Daxue Xuebao (Ziran Kexue yu Gongcheng Jishu Ban)/
Journal of Tianjin University Science and Technology
ISSN (Online):0493-2137
E-Publication: Online Open Access
Vol: 57 Issue: 03:2024
DOI: 10.5281/zenodo.10792408

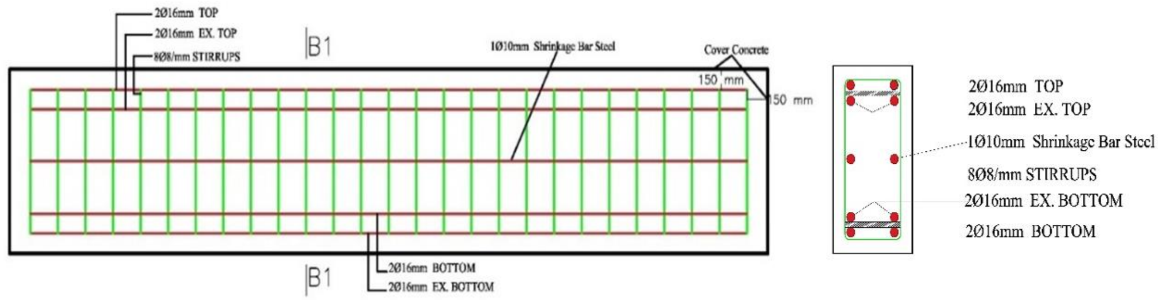

Elevation View **Cross section.**

Fig .3: Geometry and reinforcement of beam (units: mm).

Table 4: Material contents for each mix in [NSC-SC]-[HSC-SC].

Target f_{cu} at 28 days (MPa)		Mix¹(25)	Mix² (30)	Mix³ (45)	Mix⁴ (55)
Ordinary Portland cement (kg/m³)		350	400	480	520
Fine aggregate (Sand) (kg/m³)		625	633	665	680
Coarse aggregate (kg/m³)	0	675	680	620	630
	1	620	500	470	495
Water (kg/m³)		160	180	164	143
w/c		0.55	0.45	0.34	.275
Sikament R4PN (L/m³)		--	5	6	6.5
Sika ViscoCrete -3425 (L/m³)		6.3	7.2	8.6	9.3
Slump (cm)		17.2	18.9	17.2	16.4
Mean f_{cu} at 28 days (MPa)		27.2	34.1	47.6	56.7

2.4 Specimen Instrumentation and Test Procedure

Dial gauges were used to measure the lateral and vertical deflections at mid-span and quarter-span with an accuracy of 0.01 mm as shown in **Fig. 4**. The load was carefully transferred to avoid eccentricity.

After 15 to 20 load steps, the beams were gradually loaded and the expected failure occurred. When the beams were loaded to failure, a full set of deflection data was obtained using dial gauges. The failure mode and failure load were noteworthy.

A total of 10 high-strength, self-compacted, slender reinforced concrete beams were tested under static loading in the Civil Engineering Laboratory at the Faculty of Engineering, Assiut University. **Table 1** shows the dimensions of the test specimens and the details of the reinforcement.

The ends of the beams were allowed to only be supported in the horizontal and vertical planes while being torsionally constrained. Two-point loads were applied symmetrically

Tianjin Daxue Xuebao (Ziran Kexue yu Gongcheng Jishu Ban)/
Journal of Tianjin University Science and Technology
ISSN (Online):0493-2137
E-Publication: Online Open Access
Vol: 57 Issue: 03:2024
DOI: 10.5281/zenodo.10792408

to the beams at mid-span points. The test configuration **(Fig. 5)** was notably dissimilar from what other researchers had done.

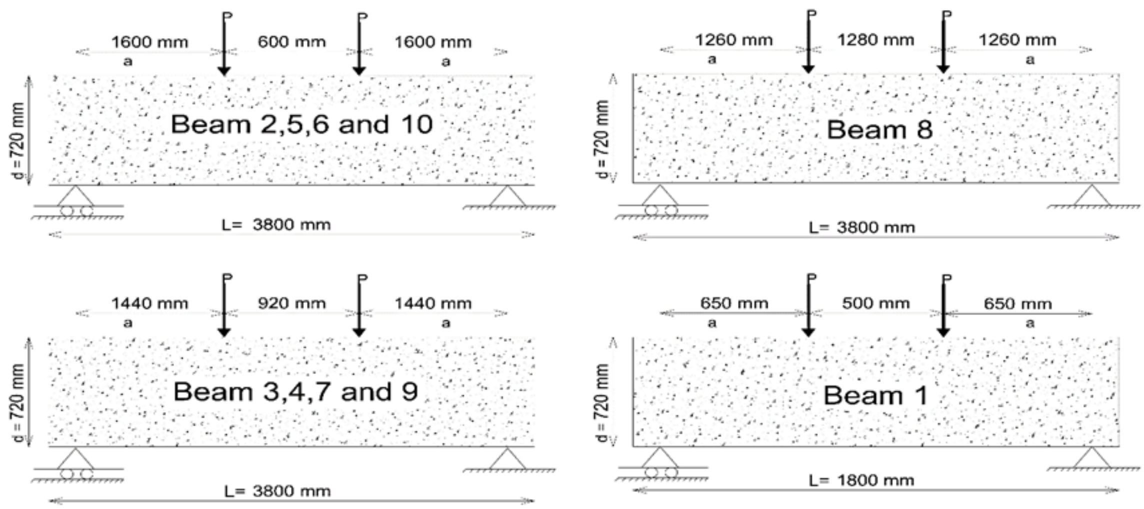

Fig. 4: Locations of loading for beams.

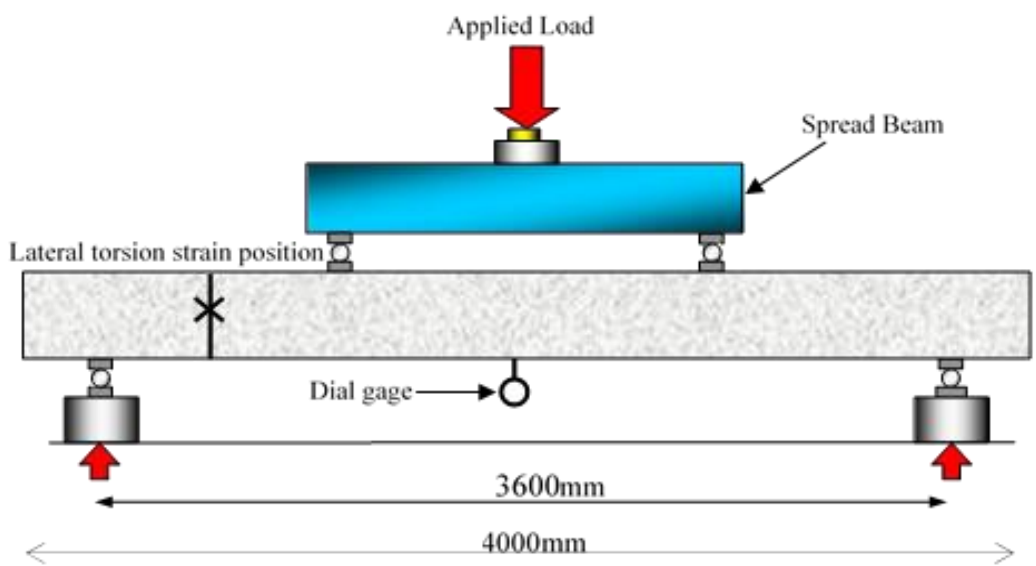

Fig. 5: Arrangement of the test specimen.

3. RESULTS AND DISCUSSIONS

Test results of high-strength self-compacted reinforced concrete for slender beams are reported. The effects of the main parameters on the behaviour of this type of beam are investigated. The results include the ultimate loads, crack patterns and failure modes obtained, load-deflection curves, load-side torsion curves, load-strains for concrete and rebars.

Tianjin Daxue Xuebao (Ziran Kexue yu Gongcheng Jishu Ban)/
Journal of Tianjin University Science and Technology
ISSN (Online):0493-2137
E-Publication: Online Open Access
Vol: 57 Issue: 03:2024
DOI: 10.5281/zenodo.10792408

3.1 Ultimate load

Figure 6 shows the impact of the ultimate load on the shear span-to-depth ratio, main reinforcement ratio, and compressive strength of the concrete. All tested cylinder beams had ultimate load less than the control beam (non-cylinder beam) by range 15% - 38 %. The ultimate load of the ideal beam (B1) was 65t. The group of beams B2, B5, B6 with concrete compressive strength equal 30, 45, and 55MPa, respectively, had ultimate load equal 45, 50, and 55t, respectively. This result was confirmed from the **Fig. 6** (a) that increasing concrete compressive strength increased the ultimate load by 9% and 18%. This is due to that higher concrete compressive strength can withstand greater compressive stresses and resist deformation under applied loads, resulting in higher load-carrying capacity. Beams made with higher concrete compressive strength exhibit greater stiffness and rigidity, which helps in distributing the applied loads more efficiently. This improved load transfer capability reduces the chances of premature failure and allows the beam to carry higher loads before reaching its ultimate limit. Beams B3, B4, and B7 which varied in main reinforcement had ultimate load equal 50, 45, and 40t. It was clear that increasing the main reinforcement ratio led to increase the ultimate load by 10% in case of B4 compared to B3 and 20% in case of B7 compared to B3. This is because a higher amount of steel reinforcement increases the tensile strength and ductility of the beam, allowing it to resist higher bending moments and shear forces. The main reinforcement plays a critical role in distributing and carrying the applied loads. It helps to control the formation and propagation of cracks in the concrete and provides additional resistance against tensile and shear stresses. By increasing the amount of reinforcement, the beam's capacity to withstand deformation and failure is enhanced, resulting in an increased ultimate load capacity. However, in the case of B4 with a higher main reinforcement ratio, it was found that the ultimate load was reduced. This is because excessive reinforcement can lead to congestion, making it difficult for the concrete to flow and causing complications during construction. Moreover, increasing the shear span-to-depth ratio led to decrease the ultimate load by 18% in case of B9 compared to B8 and 27% in case of B10 compared to B8. This is because a higher shear span-to-depth ratio leads to a higher shear demand along the beam length. When the shear span-to-depth ratio exceeds a certain limit, the beam becomes more prone to shear failure. In beams with a low shear span-to-depth ratio, such as deep beams, the concrete compression struts develop along the shear span, leading to a more efficient load transfer mechanism and higher ultimate load capacity. However, as the shear span-to-depth ratio increases, the efficiency of the compression struts decreases, resulting in reduced load-carrying capacity. **Table 5** represents the ultimate load and the cracking load for all tested beams.

Tianjin Daxue Xuebao (Ziran Kexue yu Gongcheng Jishu Ban)/
Journal of Tianjin University Science and Technology
ISSN (Online):0493-2137
E-Publication: Online Open Access
Vol: 57 Issue: 03:2024
DOI: 10.5281/zenodo.10792408

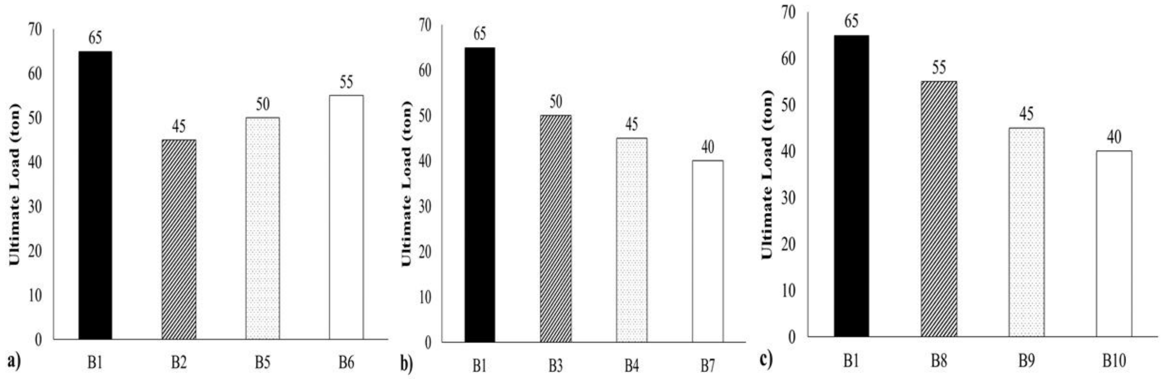

a) Effect of concrete compressive strength,

b) Effect of main reinforcement ratio, and

c) shear span-to-depth ratio.

Fig. 6: The ultimate load for tested beams:

Table 5: Results of the ultimate load and the first cracking load.

Beam label	First Crack (P_{cr}) (ton)	Ultimate load and failure (P_{uexp}) (ton)
Beam 1	14	65
Beam 2	8.5	45
Beam 3	4	50
Beam 4	3	45
Beam 5	9	50
Beam 6	10	55
Beam 7	12	40
Beam 8	2	55
Beam 9	6.5	45
Beam 10	9.5	40

3.2 Load vs. mid-span deflection

The results of load versus mid-span deflection curves for all tested beams are shown in **Figs 7 to 9**. From the plotted results, it can be concluded that the main reinforcement ratio had a notable effect on the mid-span deflection of slender beams. As the main reinforcement ratio increases, the mid-span deflection of slender beams generally decreases. This is because a higher amount of reinforcement increases the stiffness and rigidity of the beam, providing enhanced resistance against deformation under applied loads. The main reinforcement serves to control and limit the amount of deflection in the beam by restricting the development and propagation of cracks. It helps to distribute the applied loads more efficiently, reducing the magnitude of deflections and ensuring a more rigid structural response. **Beam 7** with the lowest main reinforcement ratio had the highest mid-span deflection. On the other hand, **beam 3** with higher main reinforcement ratio showed better performance. The curves of load versus mid-span deflection were linear until loads equal. Unlike, in the case of **beam 4** increasing the main reinforcement ratio

Tianjin Daxue Xuebao (Ziran Kexue yu Gongcheng Jishu Ban)/
Journal of Tianjin University Science and Technology
ISSN (Online):0493-2137
E-Publication: Online Open Access
Vol: 57 Issue: 03:2024
DOI: 10.5281/zenodo.10792408

led to decreasing the ultimate load and increasing the mid-span deflection. This can be explained by that beyond a certain point, adding excessive reinforcement may lead to congestion, making it difficult for the concrete to flow and complicating construction. So, it is important to note that while increasing the main reinforcement ratio can help reduce mid-span deflections, there is an optimal range that needs to be considered.

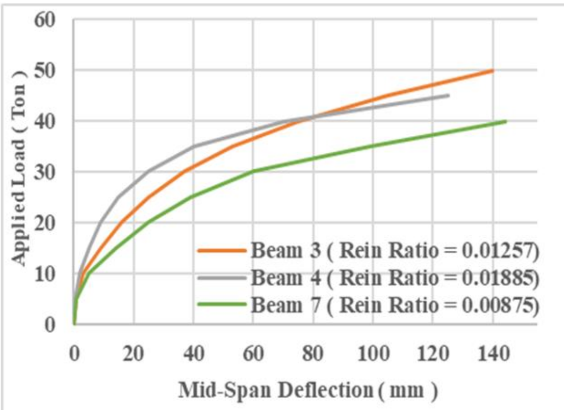

Fig. 7 Load-Deflection for beams with reinforcement ratio (%).

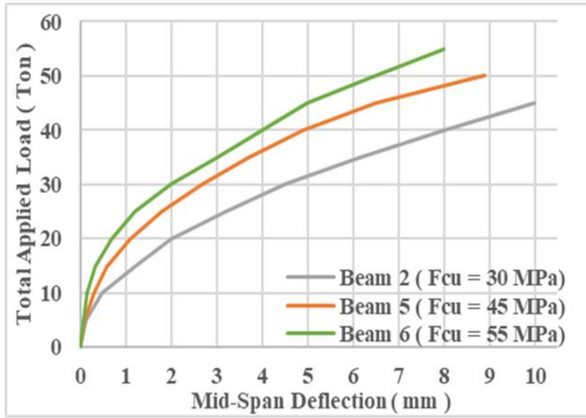

Fig. 8 Load-Deflection for beams with different concrete strength (f_{cu}).

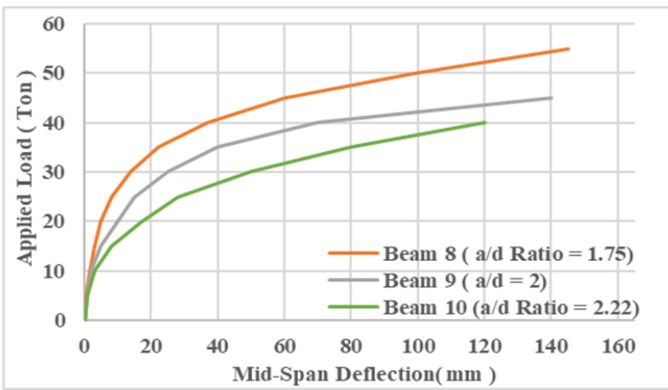

Fig. 9 Load-Deflection for beams with shear span to depth ratio *(a/d)*.

Other factors such as the concrete compressive strength, and shear span-to-depth ratio also influence the mid-span deflection. **Figures 7,8** and **9** represents the significant effect of the concrete compressive strength on the load-mid span deflection curve. It was evident that a decrease in mid-span deflection occurred as the concrete's compressive strength was increased by 20% in the case of **B6** with f_c =55 *MPa* compared to **B2** with f_c=30 *MPa*. This is due to that higher concrete compressive strength exhibits greater stiffness and rigidity, enabling it to resist deformation under applied loads more effectively. By using concrete with higher compressive strength, the beam became more capable of withstanding compressive stresses, leading to smaller deflections in the mid-span region. The increased stiffness of the high-strength concrete allowed for more efficient load distribution and limits the magnitude of deflection. Furthermore, higher concrete compressive strength improved durability and resistance to creep and shrinkage. This additional resistance helps to further minimize deflections over time, enhancing the long-term performance of the slender beams.

The shear span-to-depth ratio has a great effect on the mid-span deflection of slender beams. As the shear span-to-depth ratio increased, the mid-span deflection of slender beams generally increased. A higher shear span-to-depth ratio implies that a larger portion of the beam is subjected to shear forces, leading to an increased susceptibility to deflection. When the shear span-to-depth ratio is small, the beam experiences a more efficient load transfer mechanism through compression struts, resulting in reduced deflections. In contrast, when the shear span-to-depth ratio is large, the load transfer mechanism is less efficient, and the beam is more prone to greater mid-span deflections. The shear span-to-depth ratio affects the distribution of shear stresses along the beam length. A larger shear span-to-depth ratio led to a wider region of shear stress, increasing the likelihood of shear cracking, and contributing to greater deflections.

3.3 Crack patterns and modes of failure

In ideal beam **B1**, At a load of 14 t from the support point, the first diagonal shear crack was noticed. As the load increased, these cracks spread and extended. As illustrated in **Fig. 10**, the shear cracks spread and widened until the failure load of 65 t was attained. Because shear cracks did not extend to the place where the stresses were applied, tension failure T.F. constituted the mode of failure. The first crack seemed in **B2**, which had a 30 MPa compressive strength, at a load of 8.5 t. The steel bars eventually ruptured as a result of the flexural cracks expanding in width. As illustrated in **Fig. 11**, this rupture was accompanied by severe flexural cracking and spalling of the concrete at the tension zone, which widened until a failure load of 45 t was attained.

The first crack for **B5**, which had a 30 MPa compressive strength, appeared at a load of 9 t. As seen in **Fig. 12**, the cracks emigrated in the direction of the loading point, grew to the support, and multiplied and widening in this region. The specimen held up well under a 50t load before rupturing. The failure can be attributed to both strut compression failure and rupture failure.

With a compressive strength of 55 MPa, the **B3**, **B4**, **B6**, **B7**, **B8**, **B9**, and **B10** featured a crack pattern characterized by crack propagation in the tension zone. Flexural cracks began at the bottom side of the beams for **B3**, **B4**, **B6**, **B7**, **B8**, **B9**, and **B10** during the four-point loading test on the slender beam at a load of 4, 3, 10, 12, 2, 6.5, and 9.5 t, respectively; however, as seen in the following **Figs**, flexural cracks extended at a specific distance from the top of the beam.

Tianjin Daxue Xuebao (Ziran Kexue yu Gongcheng Jishu Ban)/
Journal of Tianjin University Science and Technology
ISSN (Online):0493-2137
E-Publication: Online Open Access
Vol: 57 Issue: 03:2024
DOI: 10.5281/zenodo.10792408

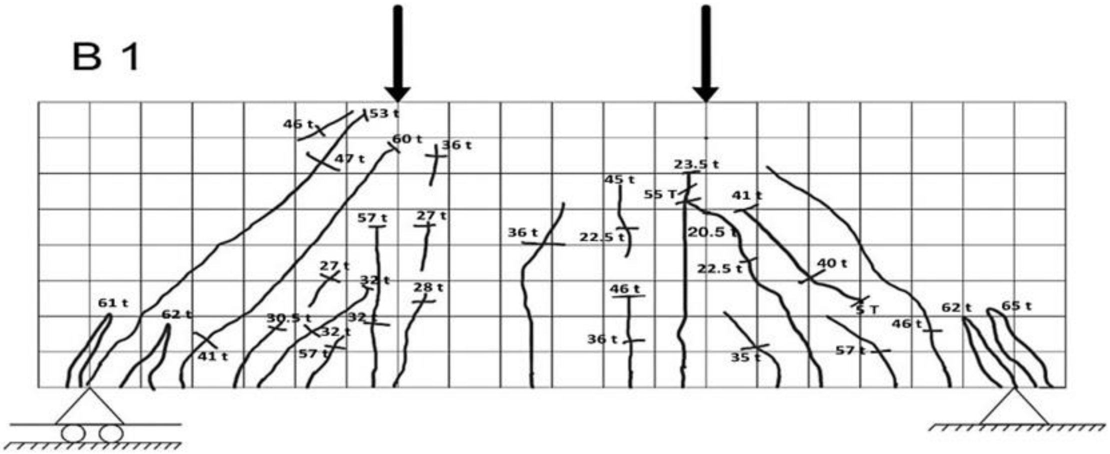

Fig. 10: The pattern of cracks in B1.

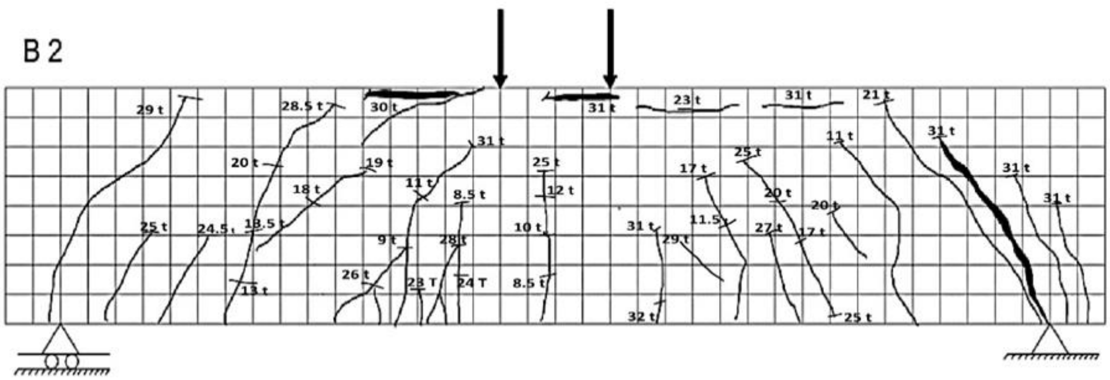

Fig. 11: The pattern of cracks in B2.

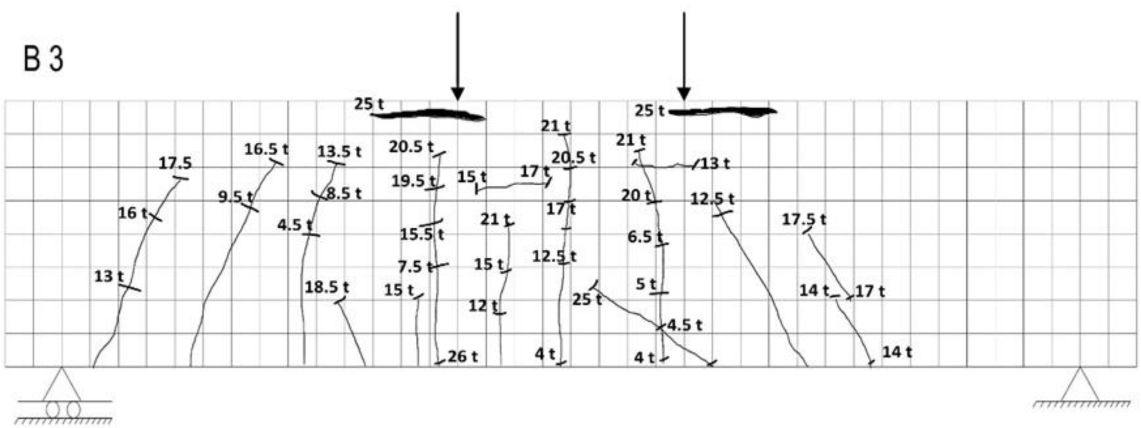

Fig. 12: The pattern of cracks in B3.

Tianjin Daxue Xuebao (Ziran Kexue yu Gongcheng Jishu Ban)/
Journal of Tianjin University Science and Technology
ISSN (Online):0493-2137
E-Publication: Online Open Access
Vol: 57 Issue: 03:2024
DOI: 10.5281/zenodo.10792408

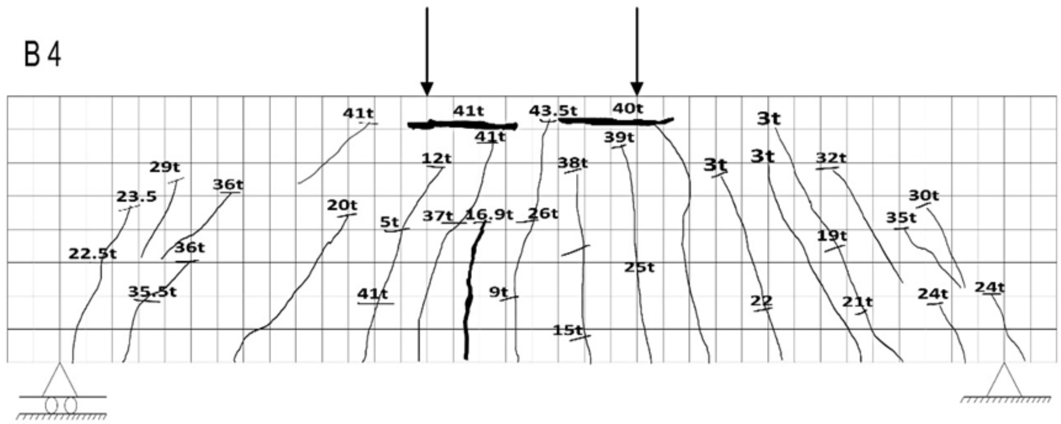

Fig. 13: The pattern of cracks in B4.

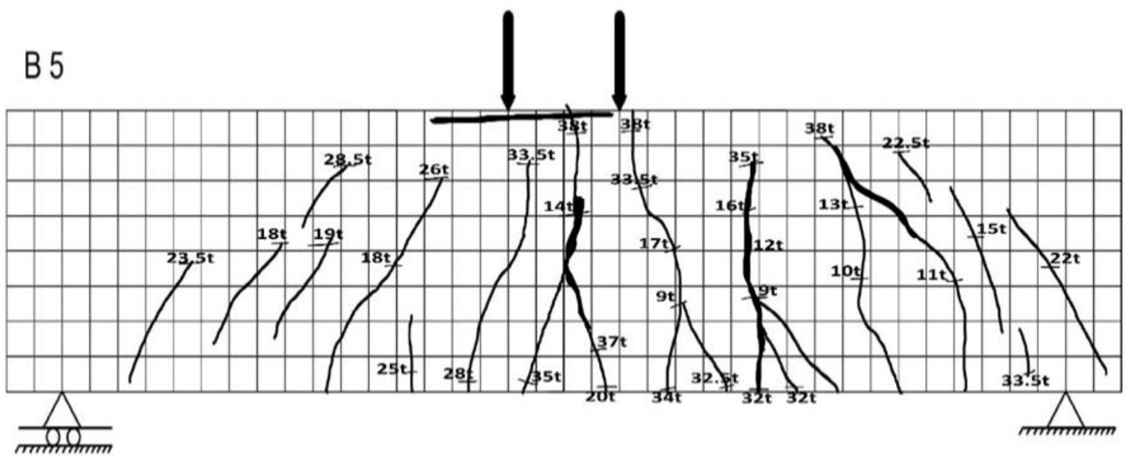

Fig. 14: The pattern of cracks in B5.

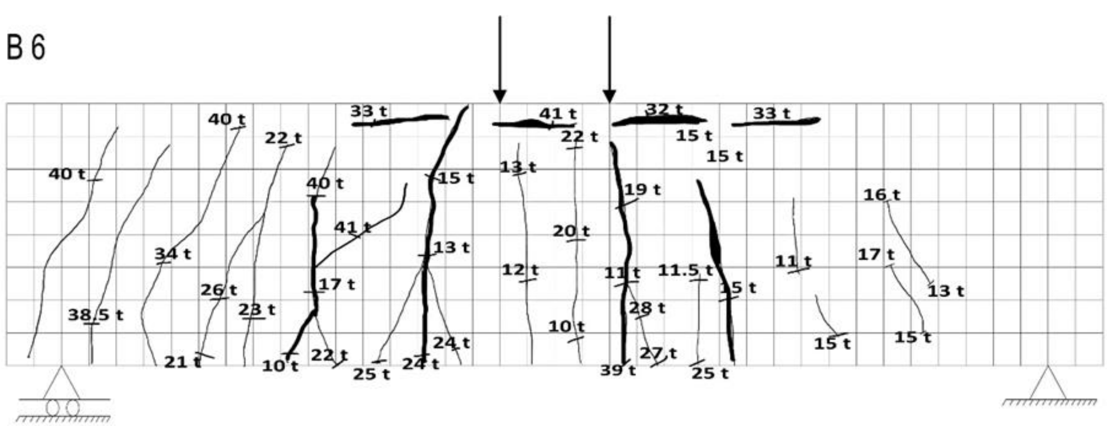

Fig. 15: The pattern of cracks in B6.

Tianjin Daxue Xuebao (Ziran Kexue yu Gongcheng Jishu Ban)/
Journal of Tianjin University Science and Technology
ISSN (Online):0493-2137
E-Publication: Online Open Access
Vol: 57 Issue: 03:2024
DOI: 10.5281/zenodo.10792408

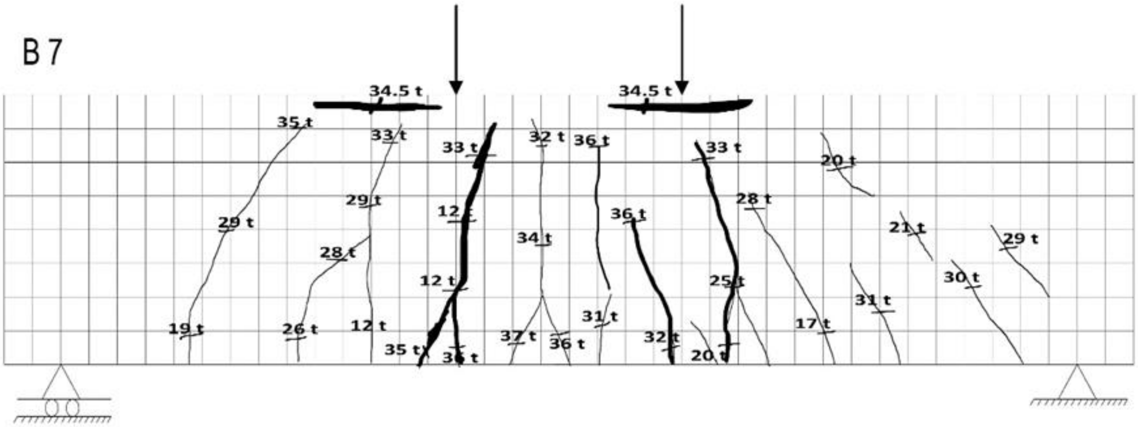

Fig. 16: The pattern of cracks in B7.

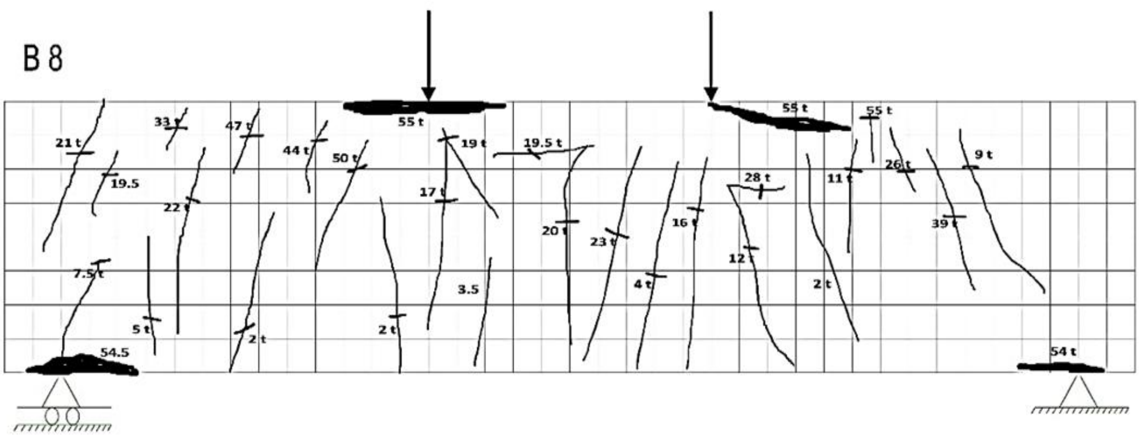

Fig. 17: The pattern of cracks in B8.

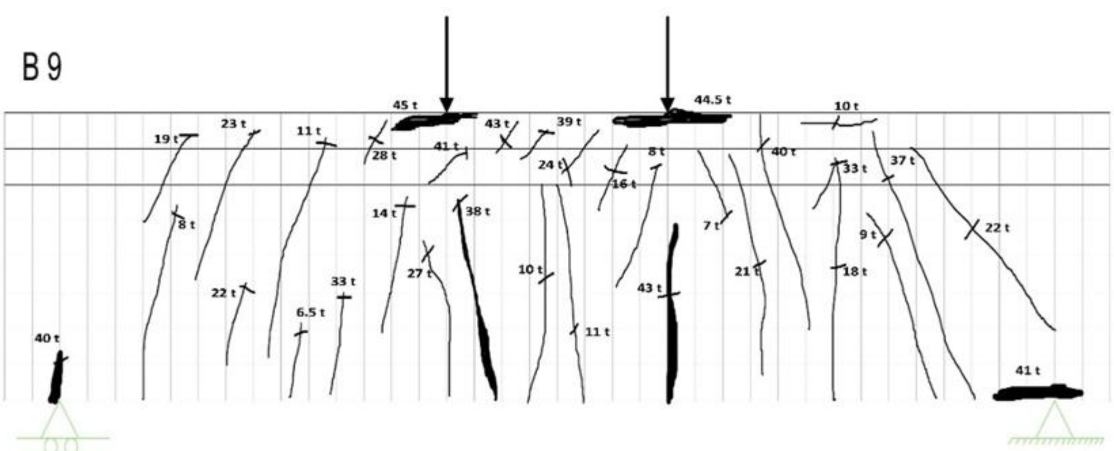

Fig. 18: The pattern of cracks in B9.

Tianjin Daxue Xuebao (Ziran Kexue yu Gongcheng Jishu Ban)/
Journal of Tianjin University Science and Technology
ISSN (Online):0493-2137
E-Publication: Online Open Access
Vol: 57 Issue: 03:2024
DOI: 10.5281/zenodo.10792408

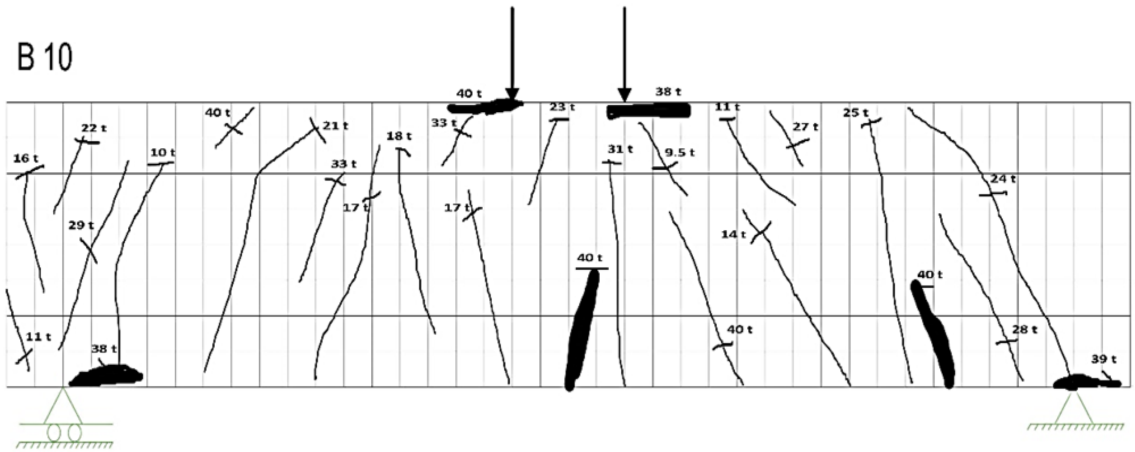

Fig. 19: The pattern of cracks in B10.

Effect of main reinforcement ratio on the crack pattern of slender beams

The effect of the main reinforcement ratio on the crack pattern of slender beams is significant. More main reinforcement ratio results in a narrower and more controlled crack pattern. This is because a higher ratio of reinforcement provides better resistance to tensile stresses, resulting in smaller crack widths and reduced crack spacing. With a higher main reinforcement ratio, the cracks tend to be more localized and confined. The increased amount of reinforcement restricts the propagation of cracks, preventing them from spreading extensively across the beam. This enhances the overall structural integrity and improves the beam's ability to withstand applied loads. On the other side, a lower main reinforcement ratio can result in wider and more widely spaced cracks. Insufficient reinforcement leads to higher tensile stresses and inadequate crack control, allowing cracks to form more freely and propagate throughout the beam. Finally, it is important to find the right balance in the main reinforcement ratio to achieve an optimal crack pattern. Excessive reinforcement can lead to congestion and practical difficulties during construction, while inadequate reinforcement may compromise the structural performance and durability of the beam.

Effect of concrete compressive strength on the crack pattern of slender beams

When the compressive strength of concrete increases with the crack pattern of slender beams tends to change. Higher concrete compressive strength exhibits greater stiffness and rigidity, which helps to control crack formation and propagation. With higher compressive strength, the concrete can withstand higher compressive stresses, reducing the likelihood of cracks forming in the first place. It provides better resistance to the tensile stresses that lead to crack initiation, resulting in a more controlled crack pattern. In addition, higher compressive strength concrete tends to exhibit greater cohesion and better bond strength with the reinforcement. This enhanced bond between the concrete and reinforcement helps to distribute the tensile forces more efficiently, limiting crack widths and minimizing crack propagation. Conversely, lower compressive strength

Tianjin Daxue Xuebao (Ziran Kexue yu Gongcheng Jishu Ban)/
Journal of Tianjin University Science and Technology
ISSN (Online):0493-2137
E-Publication: Online Open Access
Vol: 57 Issue: 03:2024
DOI: 10.5281/zenodo.10792408

concrete is more susceptible to cracking, especially under applied loads that exceed its capacity. It may exhibit wider and more extensive cracking, compromising the structural integrity of the beam.

Effect of shear span to depth ratio on the crack pattern of slender beams

The shear span-to-depth ratio has a significant effect on the crack pattern of slender beams. As the shear span-to-depth ratio increases, the crack pattern of slender beams tends to change. A higher shear span-to-depth ratio leads to a more distributed and wider crack pattern. This is because a larger shear span-to-depth ratio results in increased shear forces along the beam, which can cause the formation of multiple cracks that extend across a wider region. In beams with a low shear span-to-depth ratio, the shear forces are more concentrated near the supports. This leads to a more localized crack pattern, typically near the support regions. The cracks are narrower and tend to propagate vertically along the beam. However, as the shear span-to-depth ratio increases, the shear forces become more evenly distributed along the beam's length. This results in a broader distribution of cracks, with cracks forming in multiple locations along the beam. Higher shear span-to-depth ratios result in a more distributed and wider crack pattern, while lower ratios lead to a more localized crack pattern near the supports.

3.1 Load-Lateral Torsion Response

Figs. 20, 21, and **22** present the typical torsional moment diagram of the beams examined in this work. Although the beams are restricted, the area around the laterally supported beam ends had higher torsional moments. With the start of the testing machine, the load began to increase gradually, and the relationship between load–lateral torsion was linear in the pre-crack stage. According to the parameters previously mentioned, It is noted that **B4**, has less lateral torsion than the other beams (**B3** and **B7**), B6 has less lateral torsion than the other beams (**B2** and **B5**) and **B8** has less lateral torsion than the other beams (**B9** and **B10**).

For **beams** 3, 4, and 7, the increase in the reinforcement ratio leads to a decrease in lateral torsion by 14%. As well, for beams 2, 5, and 6, the increase in the concrete strength leads to a decrease in lateral torsion by 56% for beams 8, 9, and 10, the increase in the shear span to depth ratio *(a/d)* leads to an increase in lateral torsion by 11%.

3.2 Concrete Strain Response

Figures 23 and 24 show values of concrete strains were recorded. It is evident that the highest concrete compressive strain for beams that was measured exceeded the crushing strain of 0.003 that was stipulated by ACI 318 and ECP 203. It can be found that the concrete strain values of the beams (**B6** and **B8**) were much higher than others beam for the same load value.

An improvement in concrete's strength from 30 to 55 MPa can significantly delay the appearance of cracks in the beams For beams 2, 5, and 6 by 18%. For beams **8**, **9**, and **10**, Shear span to depth ratio (a/d) increases causing an increase in the appearance of cracks for beams by 24%.

ISSN (Online):0493-2137
E-Publication: Online Open Access
Vol: 57 Issue: 03:2024
DOI: 10.5281/zenodo.10792408

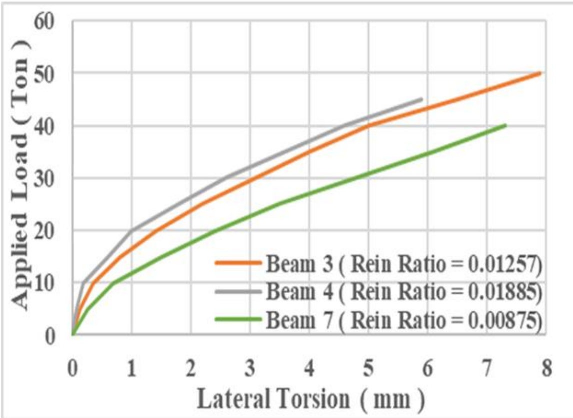

Fig.20: Load-Lateral torsion for beams with reinforcement ratio (%).

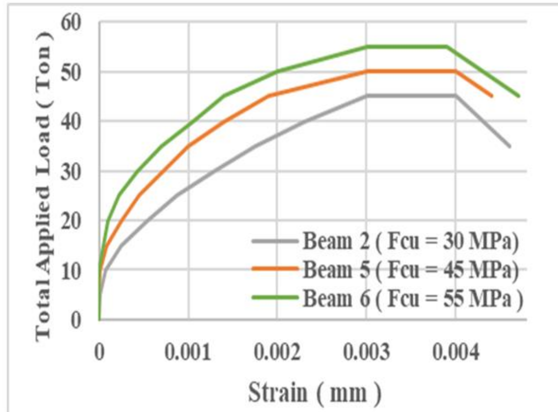

Fig.21: Load-Lateral torsion for beams with concrete strength.

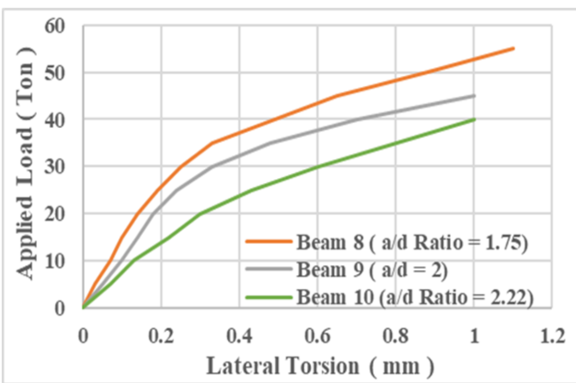

Fig.22: Load-Lateral torsion for beams with shear span to depth ratio

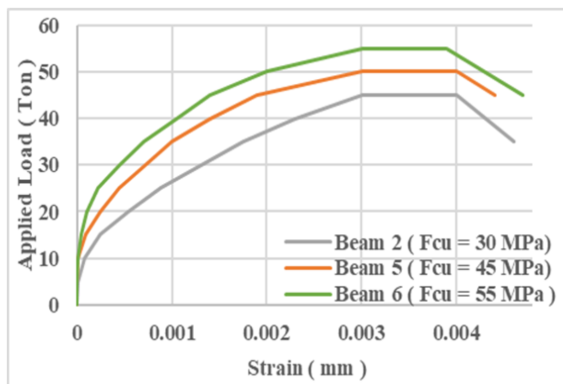

Fig. 23: Load-Concrete strain for beams B2,B5 and B6.

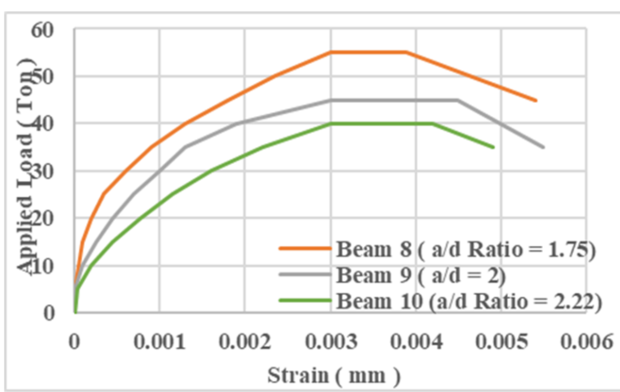

Fig. 24 Load-Concrete strain for beams B8,B9 and B10.

Tianjin Daxue Xuebao (Ziran Kexue yu Gongcheng Jishu Ban)/
Journal of Tianjin University Science and Technology
ISSN (Online):0493-2137
E-Publication: Online Open Access
Vol: 57 Issue: 03:2024
DOI: 10.5281/zenodo.10792408

3.3 Load- Strain of Main Steel Response (Tension)

On the longitudinal bars of the beam, the strain was placed. The following Figs explain the strain behavior for the tested. According to **Fig 25**, we found that the strain value of B4 is less than that of beams 3 and 7, as it contains the highest percentage of reinforcing steel. As well as **Fig 26**, we found that the strain value of B6 is less than B2 and B5, which contain the lower strength in concrete. Also, in **Fig 27**, we found that B 8 which have an *a/d* = 1.75 have fewer strain values than beams 9 and 10.

For beams 3, 4, and 7, the increase in the reinforcement ratio leads to a decrease in strain values by 2%. Also, for beams 2, 5, and 6, the increase in the concrete strength leads to a decrease in strain values by 11%. Finally, for beams 8, 9, and 10, the increase in the shear span to depth ratio *(a/d)* leads to an increase in strain values by 83%.

3.4 Load- Strain of Stirrups Response

The measured strain of steel stirrups for tested beams is shown in **Figs. 28, 29 and 30**. The strain stirrups values in all tested beams did not exceed the yielding strain before final failure. It is found from **Fig. 28**, that the strain values of beams (B3, B4 and B7) fluctuated around zero before the applied load reached around (4, 3 and 12 tons) (the major flexure crack occurred in this section at the loading level). According to these **Figures**, we found that B7 is higher in strain values than B3 and B4). Similarly, it is noted that B6 and B8 which contains the highest percentage of concrete strength (55 MPa) and *a/d* = 1.75 respectively, have fewer strain values than other beams as shown in **Fig. 29** and **30**.

For beams 3, 4, and 7, the increase in the reinforcement ratio leads to a decrease in strain values by 26%. Also, for beams 2, 5, and 6, the increase in the concrete strength leads to a decrease in strain values by 19%. Finally, for beams 8, 9, and 10, An 80% increase in strain values results from an increase in the shear span to depth ratio (a/d).

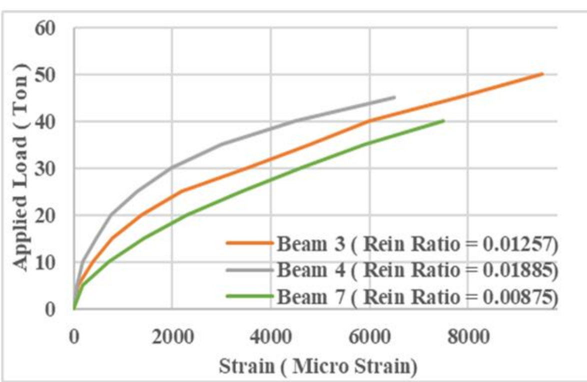

Fig. 25: Load-Steel bar strain for beams B3,B4 and B7

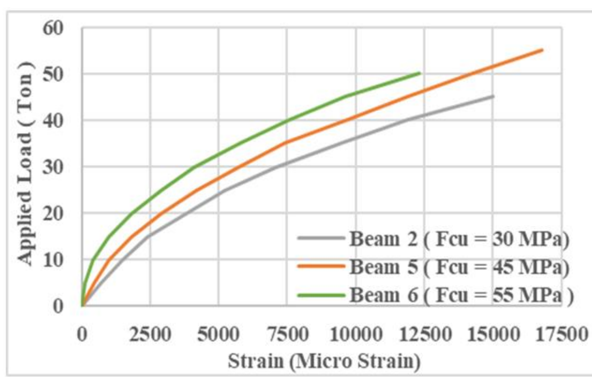

Fig. 26: Load-Steel bar strain for beams B2,B5 and B6

Tianjin Daxue Xuebao (Ziran Kexue yu Gongcheng Jishu Ban)/
Journal of Tianjin University Science and Technology
ISSN (Online):0493-2137
E-Publication: Online Open Access
Vol: 57 Issue: 03:2024
DOI: 10.5281/zenodo.10792408

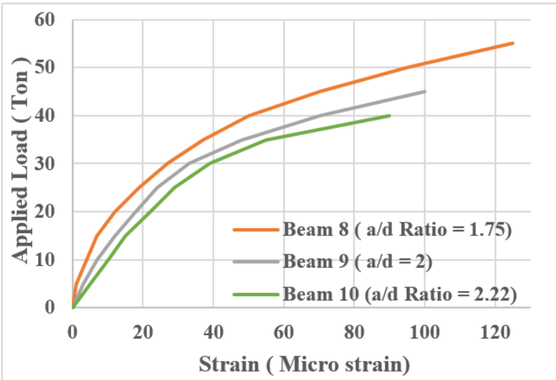

Fig. 27: Load-Steel bar strain for beams B8,B9 and B10

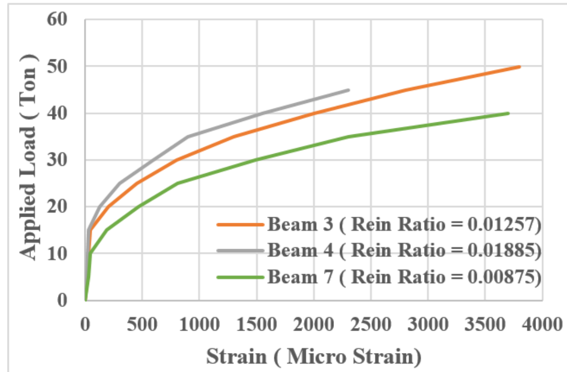

Fig. 28: Load-Stirrups strain for beams B3,B4 and B7

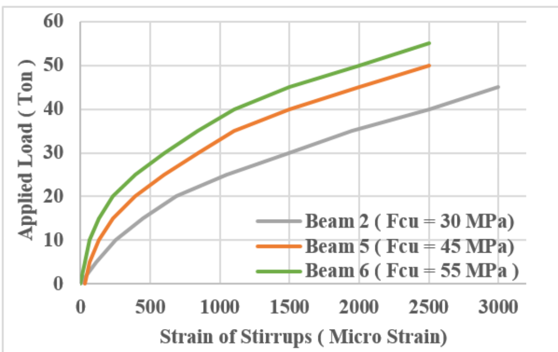

Fig 29: Load-Stirrups strain for beams B2,B5 and B6

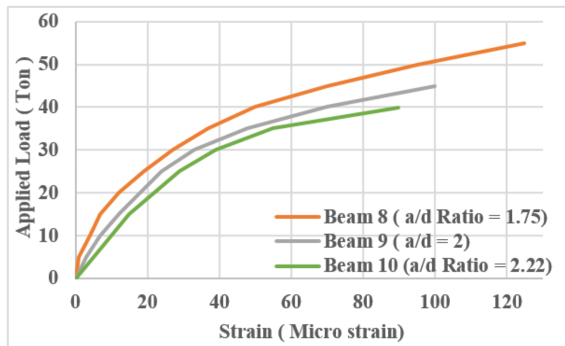

Fig 30: Load-Stirrups strain for beams B8,B9 and B10

4. CONCLUSIONS

In conclusion, the behavior of slender beams in reinforced concrete structures is influenced by various factors and parameters. Several key observations can be made regarding their behavior:

Shear Span-to-Depth Ratio: The shear span-to-depth ratio significantly affects the shear strength, deflection, and crack pattern of slender beams. Higher ratios result in more distributed shear forces, wider cracks, and reduced shear strength.

1. Concrete Compressive Strength: The concrete compressive strength plays a crucial role in the overall behavior of slender beams. Higher compressive strength leads to improved crack control, increased stiffness, and enhanced resistance against deformation and failure.
2. Main Reinforcement Ratio: The main reinforcement ratio influences the cracking behavior, load-carrying capacity, and deflection of slender beams. Higher

reinforcement ratios result in more controlled crack patterns, increased load-bearing capacity, and improved structural performance.

3. It is important to note that these factors are interrelated and must be considered in conjunction with each other to achieve optimal behavior and performance of slender beams. The selection of appropriate parameters, such as the shear span-to-depth ratio, concrete compressive strength, and main reinforcement ratio, requires careful consideration to ensure adequate structural integrity, crack control, and load-carrying capacity.
4. In summary, understanding the behavior of slender beams is crucial for the design and analysis of reinforced concrete structures. By considering factors such as the shear span-to-depth ratio, concrete compressive strength, and main reinforcement ratio, engineers can optimize the behavior of slender beams, ensure structural integrity, and meet design requirements for safety and performance.

Acknowledgements

Authors are thankful to Department of Civil Engineering, Aswan university to support this study.

Declarations

Conflict of interest. The authors declare that none of the work reported in this study could have been influenced by any known competing financial interests or personal relationships.

Author Contributions

Author Contributions Mohamed Elsibaey was involved in conceptualization, writing—review and editing, supervision, and investigation. The remaining authors contributed to the methodology, writing, and original draft.

References

[1] J. K. Wight and J. G. MacGregor, *Reinforced concrete*. England: Pearson Education Limited UK, 2016.

[2] S.-G. Hong, N. K. Hong, and S.-K. Jang, "Deformation Capacity of Structural Concrete in Disturbed Regions," *ACI Structural Journal,* vol. 108, 2011.

[3] J. Barry and H. Ainso, "Single-span deep beams," *Journal of Structural Engineering,* vol. 109, pp. 646-663, 1983.

[4] A. B. Matamoros and K. H. Wong, "Design of simply supported deep beams using strut-and-tie models," 2003.

[5] K.-H. Yang, H.-S. Chung, E.-T. Lee, and H.-C. Eun, "Shear characteristics of high-strength concrete deep beams without shear reinforcements," *Engineering structures,* vol. 25, pp. 1343-1352, 2003.

[6] N. C. Roy and S. F. Brena, "Behavior of deep beams with short longitudinal bar anchorages," *ACI Structural Journal,* vol. 105, p. 460, 2008.

[7] K.-H. Yang, "Tests on Lightweight Concrete Deep Beams," *ACI Structural journal,* vol. 107, 2010.

[8] A. Arabzadeh, R. Aghayari, and A. R. Rahai, "Investigation of experimental and analytical shear strength of reinforced concrete deep beams," 2011.

[9] I. Shaaban, F. Beshara, and T. Mustafa, "Behaviour of Reinforced Concrete Continuous Deep Beams in Shear," *Engineering Research Journal, Benha University, Vol. 17,* 2012.

[10] I. Shaaban, F. Beshara, and T. Mustaf, "Behaviour and analysis of reinforced concrete continuous deep beams," *http://str. eng. cu. edu. eg/wp-content/uploads/sites/6/str1/2017/ASEC12-in-Libya-2013-Brochure-English-version. pdf,* 2013.

[11] A. R. Mohamed, M. S. Shoukry, and J. M. Saeed, "Prediction of the behavior of reinforced concrete deep beams with web openings using the finite element method," *Alexandria Engineering Journal,* vol. 53, pp. 329-339, 2014.

[12] H. Chen, W.-J. Yi, and Z. J. Ma, "Shear size effect in simply supported RC deep beams," *Engineering Structures,* vol. 182, pp. 268-278, 2019.

[13] A. Committee, "Building code requirements for structural concrete (ACI 318-08) and commentary," 2008.

[14] ACI, "ACI concrete mix design," *American concrete institute , ACI 211, revision 613-54.*

[15] A. Ashour and K. H. Yang, "Application of plasticity theory to reinforced concrete deep beams: a review," *Magazine of Concrete Research,* vol. 60, pp. 657-664, 2008.

[16] A. H. Gandomi, A. H. Alavi, S. Kazemi, and M. Gandomi, "Formulation of shear strength of slender RC beams using gene expression programming, part I: Without shear reinforcement," *Automation in Construction,* vol. 42, pp. 112-121, 2014.

[17] F. Beshara, I. Shaaban, and T. Mustafa, "Strut-and-Tie modelling of RC continuous deep beams," in *ASEC 2015 Conference in Algeria*, 2015, pp. 12-15.

[18] M. Shahnewaz, A. Rteil, and M. S. Alam, "Shear strength of reinforced concrete deep beams–A review with improved model by genetic algorithm and reliability analysis," in *Structures*, 2020, pp. 494-508.

[19] D.-C. Feng, W.-J. Wang, S. Mangalathu, G. Hu, and T. Wu, "Implementing ensemble learning methods to predict the shear strength of RC deep beams with/without web reinforcements," *Engineering Structures,* vol. 235, p. 111979, 2021.

[20] B. Chen, J. Zhou, D. Zhang, J. Su, C. Nuti, and K. Sennah, "Experimental study on shear performances of ultra-high performance concrete deep beams," in *Structures*, 2022, pp. 310-322.

[21] I. Standard, "Code of practice for plain and reinforced concrete," *Bureau of Indian Standard, New Delhi, India,* 2000.

[22] A. Standard, "Concrete structures," *AS-3600. Sydney: Standards Australia International,* 2001.

[23] E. C. f. D. a. C. o. R. C. Structures, "ECP 203- 2018," 2018.

[24] W. Hansell and G. Winter, "Lateral Stablity of Reinforced Concrete Beams," in *Journal Proceedings*, 1959, pp. 193-214.

[25] A. Siev, "The lateral buckling of slender reinforced concrete beams," *Magazine of Concrete Research,* vol. 12, pp. 155-164, 1960.

[26] J. K. Sant and R. W. Bletzacker, "Experimental study of lateral stability of reinforced concrete beams," in *Journal Proceedings*, 1961, pp. 713-736.

[27] K. Girija and D. Menon, "Reduction in flexural strength in rectangular RC beams due to slenderness," *Engineering Structures,* vol. 33, pp. 2398-2406, 2011.

[28] B. Kolhapure, "Shear behavior of reinforced concrete slender beams using high-strength concrete," *International Journal of Research in Engineering and technology,* pp. 79-84, 2013.

[29] S. Perera, L. H. Quang, H. Mutsuyoshi, and H. Minh, "Shear Behavior of Reinforced Concrete Beams Using High-Strength Concrete," *Proc. of Japan Concrete Institute (JCI),* vol. 31, pp. 589-594, 2009.

Tianjin Daxue Xuebao (Ziran Kexue yu Gongcheng Jishu Ban)/
Journal of Tianjin University Science and Technology
ISSN (Online):0493-2137
E-Publication: Online Open Access
Vol: 57 Issue: 03:2024
DOI: 10.5281/zenodo.10792408

[30] R. S. Pendyala and P. Mendis, "Experimental study on shear strength of high-strength concrete beams," *Structural Journal,* vol. 97, pp. 564-571, 2000.

[31] S. Construction, "<Sikament R4PN.pdf>," *Sika Construction,* vol. 1, pp. 1-2, 2016 2016.

[32] S. Construction, "<Sika ViscoCrete® -3425.pdf>," *Sika Construction,* vol. 12, pp. 1-2, 2015.